AGU PUBLICATIONS

JGR

Journal of Geophysical Research: Atmospheres

RESEARCH ARTICLE
10.1002/2015JD024671

Key Points:
- Complex responses of aerosols to NO_x emissions were simulated by a gas-aerosol coupling model
- Aerosol sensitivity to emissions was enhanced by inclusion of OA formation and BC aging processes
- NO_x emissions made a large contribution to the enhancement of aerosol parameters from 1850 to 2000

Supporting Information:
- Supporting Information S1

Correspondence to:
H. Matsui,
matsui@nagoya-u.jp

Citation:
Matsui, H., and M. Koike (2016), Enhancement of aerosol responses to changes in emissions over East Asia by gas-oxidant-aerosol coupling and detailed aerosol processes, *J. Geophys. Res. Atmos.*, *121*, 7161–7171, doi:10.1002/2015JD024671.

Received 17 DEC 2015
Accepted 10 MAY 2016
Accepted article online 14 MAY 2016
Published online 24 JUN 2016

Enhancement of aerosol responses to changes in emissions over East Asia by gas-oxidant-aerosol coupling and detailed aerosol processes

H. Matsui[1,2,3] and M. Koike[4]

[1]Graduate School of Environmental Studies, Nagoya University, Nagoya, Japan, [2]Department of Earth and Atmospheric Sciences, Cornell University, Ithaca, New York, USA, [3]Department of Environmental Geochemical Cycle Research, Japan Agency for Marine-Earth Science and Technology, Yokohama, Japan, [4]Department of Earth and Planetary Science, Graduate School of Science, University of Tokyo, Tokyo, Japan

Abstract We quantify the responses of aerosols to changes in emissions (sulfur dioxide, black carbon (BC), primary organic aerosol, nitrogen oxides (NO_x), and volatile organic compounds) over East Asia by using simulations including gas-oxidant-aerosol coupling, organic aerosol (OA) formation, and BC aging processes. The responses of aerosols to NO_x emissions are complex and are dramatically changed by simulating gas-phase chemistry and aerosol processes online. Reduction of NO_x emissions by 50% causes a 30–40% reduction of oxidant (hydroxyl radical and ozone) concentrations and slows the formation of sulfate and OA by 20–30%. Because the response of OA to changes in NO_x emissions is sensitive to the treatment of emission and oxidation of semivolatile and intermediate volatility organic compounds, reduction of the uncertainty in these processes is necessary to evaluate gas-oxidant-aerosol coupling accurately. Our simulations also show that the sensitivity of aerosols to changes in emissions is enhanced by 50–100% when OA formation and BC aging processes are resolved in the model. Sensitivity simulations show that the increase of NO_x emissions from 1850 to 2000 explains 70% (40%) of the enhancement of aerosol mass concentrations (direct radiative effects) over East Asia during that period through enhancement of oxidant concentrations and that this estimation is sensitive to the representation of OA formation and BC aging processes. Our results demonstrate the importance of simultaneous simulation of gas-oxidant-aerosol coupling and detailed aerosol processes. The impact of NO_x emissions on aerosol formation will be a key to formulating effective emission reduction strategies such as BC mitigation and aerosol reduction policies in East Asia.

1. Introduction

Aerosol particles in the atmosphere play an important role in the Earth's climate system, both directly (aerosol-radiation interactions) and indirectly (aerosol-cloud interactions) [*Boucher et al.*, 2013]; they can also cause a variety of human health problems [*Pope et al.*, 2002]. Effective strategies to reduce aerosols and their precursor gaseous species in the atmosphere are therefore urgently needed to address both climate and human health problems. Black carbon (BC) aerosols, which absorb solar radiation efficiently, have large positive radiative forcing. Reduction of BC emissions can reduce positive climate forcing in the short term and mitigate global warming [*Ramanathan and Xu*, 2010; *Bond et al.*, 2013]. Strategies to reduce aerosols in megacities are also needed, especially for cities in East Asia (e.g., China and India), where severe air pollution due to ozone (O_3) and aerosols occurs frequently [*Chan and Yao*, 2008].

The impacts of aerosols on climate and the responses of aerosols to emission reductions are generally evaluated by using three-dimensional (global or regional) aerosol models. Various aerosol processes, such as the transformation of BC particles by condensation and coagulation and the formation of organic aerosols (OA) and nitrate aerosols, are important in these evaluations. The absorption efficiency and the cloud condensation nuclei activity of BC particles are gradually enhanced by microphysical and chemical (aging) processes during their transport in the atmosphere [*Bond et al.*, 2006, 2013; *Stier et al.*, 2006; *Moteki et al.*, 2007]. Some aerosol models can calculate these enhancements based on condensation and coagulation [*Jacobson*, 2002; *Bauer et al.*, 2013; *He et al.*, 2016; *Liu et al.*, 2016; *Matsui*, 2016a, 2016b]. Aerosol models had severely underestimated OA formation rates and OA concentrations in the atmosphere, especially over urban areas [*Heald et al.*, 2005; *Matsui et al.*, 2009; *Utembe et al.*, 2011; *Tsigaridis et al.*, 2014], but recent studies have reported better agreement between observed and simulated OA concentrations over urban areas

[*Hodzic et al*., 2010; *Tsimpidi et al*., 2011; *Ahmadov et al*., 2012]. Many aerosol models also consider the formation of nitrate aerosols [*Xu and Penner*, 2012; *Hauglustaine et al*., 2014]. In addition, online simulations of gas-phase chemistry and aerosol processes (gas-oxidant-aerosol coupling) are important [*Shindell et al*., 2009] because oxidant species produced from nitrogen oxides (NO_x) and volatile organic compounds (VOC) change the formation rates of inorganic and organic aerosols. Many chemistry-aerosol models consider gas-oxidant-aerosol coupling [*Berglen et al*., 2004; *Bell et al*., 2005; *Fry et al*., 2012; *Yu et al*., 2013]. Because model representations of these gas and aerosol processes have improved considerably, an aerosol model that can calculate these processes should be used to evaluate the responses of aerosols to emissions. However, few aerosol models consider all these processes and improvements simultaneously.

In our previous studies, we developed an aerosol module called the Aerosol Two-dimensional bin module for foRmation and Aging Simulation (ATRAS) [*Matsui et al*., 2014a] by using the framework of the Weather Research and Forecasting and Chemistry (WRF-Chem) model with the Model for Simulating Aerosol Interactions and Chemistry (MOSAIC) aerosol module. The WRF-Chem/ATRAS-MOSAIC uses a two-dimensional bin representation (20 size bins for particles from 1 nm to 10 μm in dry diameter and up to 10 BC mixing state bins) to explicitly calculate a series of aerosol processes in the atmosphere, including OA and nitrate formation and BC aging processes and their coupling with gas-phase chemistry.

In this study, we apply the WRF-Chem/ATRAS-MOSAIC model to East Asia, one of the largest sources of aerosols and their precursors in the world. Our aerosol modeling shows that gas-oxidant-aerosol coupling, OA formation, and BC aging processes play important roles in simulations of aerosol concentrations, their radiative effects, and their responses to changes of emissions (sulfur dioxide (SO_2), BC, primary OA (POA), NO_x, and VOC) over East Asia. The model schemes and setups used in this study and the model simulations conducted in this study are described in section 2. In section 3, we elucidate the sensitivity of aerosol mass concentrations and radiative effects to reductions of primary emissions (section 3.1) and aerosol responses to emissions from the past to the future (section 3.2) by focusing on the impact of changes in NO_x emissions on aerosol parameters through gas-oxidant-aerosol coupling processes.

2. Model Schemes, Setups, and Simulations

2.1. WRF-Chem/ATRAS-MOSAIC

We use the following chemistry schemes in the WRF-Chem/ATRAS-MOSAIC model. Gas-phase chemistry and photolysis are calculated with the SAPRC-99 [*Carter*, 2000] and the Fast-J [*Wild et al*., 2000] schemes, respectively. The nucleation rate at 1 nm is calculated by using the activation-type nucleation mechanism [*Kulmala et al*., 2006] in the boundary layer and a binary homogeneous nucleation mechanism [*Wexler et al*., 1994] in the free troposphere. A coefficient of $2 \times 10^{-7}\,s^{-1}$ was adopted in the activation-type mechanism [*Matsui et al*., 2011]. Coagulation is calculated with the scheme of *Matsui et al*. [2013a], which is an extension of a semiimplicit algorithm of *Jacobson et al*. [1994]. Condensation and evaporation of sulfate and nitrate are calculated with the MOSAIC module [*Zaveri et al*., 2008]. OA formation processes are calculated with the volatility basis-set (VBS) scheme of *Matsui et al*. [2014b], which uses nine volatility classes of semivolatile and intermediate volatility organic compounds (S/IVOCs). Aqueous-phase and particle-phase OA formation processes are not considered in our model, although OA formation has the potential to be more interactive with oxidant and inorganic species when these formation processes are included in the model [*Surratt et al*., 2010; *Ervens et al*., 2011, 2014; *Liu et al*., 2012]. Aerosol activation to cloud and aqueous-phase chemistry (for inorganics) are calculated by the schemes of *Abdul-Razzak and Ghan* [2000] and *Fahey and Pandis* [2001], respectively. The shift of bins due to condensation/evaporation and coagulation is calculated based on the scheme of *Matsui et al*. [2013a]. Dry and wet deposition are calculated by using the scheme of *Easter et al*. [2004].

Optical and radiative parameters for aerosols are calculated off-line in this study [*Matsui et al*., 2013a, 2014a]. Aerosol optical properties are calculated for wavelengths of 300, 400, 600, and 999 nm using the codes of *Bohren and Huffman* [1998] by assuming the shell-core representation (BHCOAT) for internally mixed BC particles and the well-mixed representation (BHMIE) for pure-BC and BC-free particles. The shell-core assumption may overestimate/underestimate BC absorption because BC absorption is sensitive to the structure of BC and coating material [e.g., *He et al*., 2015]; however, the assumption is reasonable, at least over the outflow region in East Asia during the simulation periods [*Matsui*, 2016a]. Using the optical parameters, shortwave radiative transfer is calculated according to the Goddard scheme (a two-stream adding method based on *Chou* [1992]).

Details of the WRF-Chem/MOSAIC model are given by *Fast et al*. [2006] and *Zaveri et al*. [2008]. Details of the ATRAS model are given by *Matsui et al*. [2011, 2013a, 2013b, 2014a, 2014b].

2.2. Simulation Setups

We use the same simulation domains (outer and inner) as those used by *Matsui et al*. [2013a, 2014a] (Figure S1 in the supporting information). Horizontal grid spacings are 360 km and 120 km for the outer and inner domains, respectively, and there are 13 vertical levels from the surface to 100 hPa. The simulation period is from 21 March to 26 April 2009. We used the data over the inner domain from 24 March to 26 April for our analysis of the results. The simulations have been validated in our previous studies [*Matsui et al*., 2011, 2013a, 2013b, 2014a, 2014b] by surface and aircraft measurements over the outflow regions in East Asia [*Takami et al*., 2005, 2007; *Kanaya et al*., 2007; *Kondo et al*., 2010, 2011; *Moteki et al*., 2012; *Oshima et al*., 2012; *Takegawa et al*., 2014]: BC, sulfate, and OA mass concentrations, number concentrations of aerosols (>10 nm in diameter), BC mixing state, and O_3 and OH concentrations.

We use anthropogenic and biomass burning emissions provided by *Lamarque et al*. [2010], and their historic emissions in 2000 are used for the simulations in 2009 (section 3.1). Only these emission data are different from those used in the simulations of *Matsui et al*. [2014a]. The main conclusions obtained in this study are not changed by the choice of these emissions (Figure S2). We also use the historic emissions (from 1850 to 2000) and future emissions of the Representative Concentration Pathways (RCP) [*Moss et al*., 2010] for sensitivity simulations in section 3.2. Biogenic emissions are calculated using the Model of Emissions of Gases and Aerosols from Nature version 2 [*Guenther et al*., 2006]. Similar to previous studies [*Matsui et al*., 2013a, 2014a], emissions of dust and sea-salt particles from natural sources are not considered. Primary aerosol emissions are given as pure-BC or BC-free particles from 40 nm to 10 μm in dry diameter. They are assumed to have lognormal distributions with a median diameter of 50 nm and a standard deviation of 2.0. These assumptions are similar to those used by *Matsui et al*. [2013a, 2014a]. The parameters used in the VBS scheme are based on previous studies: the total emissions of S/IVOCs and POA are 2.5 times the POA emissions [*Tsimpidi et al*., 2010], the oxidation by OH is calculated with a rate constant of 4×10^{-11} (1×10^{-11}) $cm^3\,mol^{-1}\,s^{-1}$ for S/IVOCs from POA and oxygenated POA (for S/IVOCs from anthropogenic VOCs) [*Murphy and Pandis*, 2009], and the dry deposition velocity of S/IVOCs is assumed to be half that of nitric acid [*Ahmadov et al*., 2012]. OA concentrations simulated with these parameters are generally similar to those simulated by *Matsui et al*. [2014b] over East Asia when we use the same emission inventory.

2.3. Model Simulations

To evaluate the sensitivity of simulated aerosols to changes in emissions, we conduct sensitivity simulations by reducing the emissions for each of five emission species (SO_2, BC, POA, NO_x, and VOC) by 50% (section 3.1). We also evaluate the responses of aerosols to the changes in emissions from 1850 to 2100 by using the historic and RCP emissions; meteorological inputs in 2009 are used for these simulations (section 3.2).

We conduct model simulations with two different aerosol treatments (BASE and SIMPLE). The BASE simulations calculate all aerosol processes in the ATRAS module (including OA and nitrate formation and BC aging processes) by using a two-dimensional bin representation: 8 size bins for particles from 1 to 40 nm and 12 size and 4 BC mixing state bins for particles from 40 nm to 10 μm. The BASE simulations can treat pure-BC particles (BC mass fraction of 0.99–1.00), BC-free particles (BC mass fraction of 0), and two classes of internally mixed BC particles (BC mass fractions of 0–0.8 and 0.8–0.99). The enhancement of BC absorption efficiency by aging processes is calculated from the information of internally mixed BC particles.

The SIMPLE simulations use the aerosol representation of size-resolved only: 20 size bins from 1 nm to 10 μm in dry diameter (single mixing state for each size bin). In the SIMPLE simulations, aerosol radiative effects are calculated without OA and nitrate formation and without enhancement of BC absorption, as described below. OA formation processes are not considered in the SIMPLE simulations, and POA is treated as nonvolatile. Nitrate formation is considered in the WRF-Chem/ATRAS-MOSAIC simulations, but it is excluded in the calculations of optical and radiative parameters by setting nitrate concentrations to zero. All particles are treated as internally mixed BC particles in the WRF-Chem/ATRAS-MOSAIC simulations, but they are treated as pure BC or BC-free particles in the off-line optical calculations. In the optical calculations, particles are separated into pure BC and BC-free particles by using the method of *Matsui et al*. [2013a, 2014a], in which total

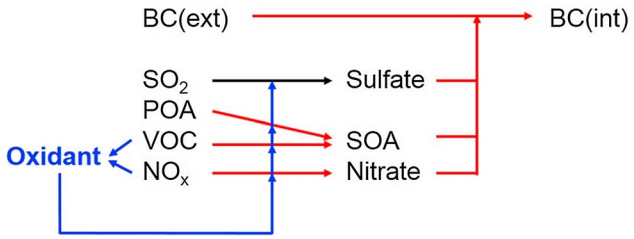

Figure 1. Schematic illustration of aerosol formation and transformation processes considered in the WRF-Chem/ATRAS-MOSAIC model. The blue arrows show the gas-oxidant-aerosol coupling processes, and the red arrows show the detailed aerosol processes such as OA and nitrate formation and BC aging processes. BC(ext) and BC(int) denote externally mixed and internally mixed BC, respectively. The red arrows from sulfate, SOA, and nitrate show the enhancement of absorption and cloud condensation nuclei activity of BC-containing particles by condensation and coagulation processes. BASE simulations consider blue, red, and black arrows. SIMPLE simulations consider only blue and black arrows.

mass concentrations of each species are conserved, but total number concentrations are doubled. Because all BC is treated as pure-BC (externally mixed BC), the optical and radiative parameters calculated in the SIMPLE simulations do not include the enhancement of BC absorption efficiency by condensation and coagulation processes.

The BASE simulations consider all processes in Figure 1 (red, blue, and black arrows), whereas the SIMPLE simulations consider only the blue and black arrows in Figure 1. Comparison of the BASE and SIMPLE simulations allows us to consider the importance of OA and nitrate formation and BC aging processes.

3. Results and Discussion

3.1. Aerosol Responses to Reductions of Emissions

Figure 2 shows the sensitivity of aerosol mass concentrations (ΔM) at an altitude of 1 km to 50% reductions of five emission species over East Asia in the BASE simulations. The emissions of S/IVOCs are treated as POA emissions (not VOC emissions) in this study. Sulfate and BC concentrations decrease almost linearly (44% for sulfate and 50% for BC) in response to 50% reductions in SO_2 and BC emissions, respectively (two left columns in Figure 2). The reduction of POA (+S/IVOCs) emissions reduces OA concentrations by 31%.

The responses to reductions of NO_x and VOC emissions are much more complex (two right columns in Figure 2). A 50% reduction of NO_x emissions considerably reduces the concentrations of sulfate (by 24%) and OA (by 30%), because oxidant concentrations are suppressed by the reduction of NO_x emissions: the concentrations of OH, HO_2, O_3, H_2O_2, and NO_3 decline by 40%, 9%, 27%, 12%, and 69%, respectively (Figure S3). The lower oxidant concentrations slow both the conversion rate of SO_2 to sulfate and the aging speed of S/IVOCs. In contrast, the reduction of VOC emissions enhances OH concentrations (by 27%) so that sulfate concentration is enhanced by 16%. The slight reduction (by 7%) of OA concentrations reflects the net effect of the reduction of VOC concentrations (lower emissions) and the faster aging speed of S/IVOCs (higher OH concentrations). In fact, anthropogenic and biogenic secondary OA (OA formed from anthropogenic and biogenic VOCs) are reduced by 30–45% due to the 50% reduction of VOC emissions, whereas oxygenated POA (OA formed from primary S/IVOCs) is enhanced by 25% because of the enhancement of OH. The responses of sulfate and OA concentrations to the changes in NO_x and VOC emissions are determined by the sensitivity of sulfate and OA schemes to oxidant concentrations in the model simulations. OA is sensitive to reductions of NO_x emissions in this study because the OA formation rate calculated by the VBS scheme is strongly

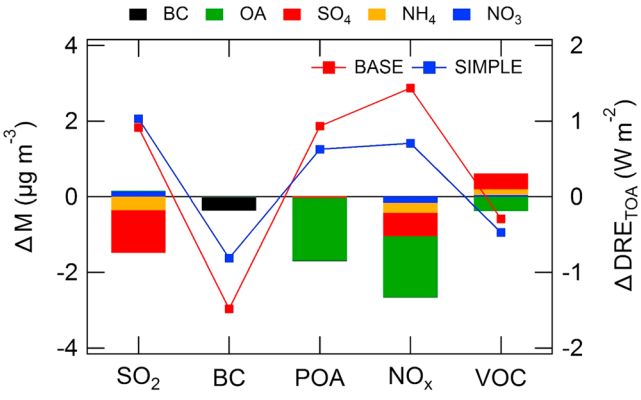

Figure 2. Sensitivity of aerosol mass concentrations (ΔM) at an altitude of 1 km and aerosol direct radiative effect at the top of the atmosphere (ΔDRE_{TOA}) to reductions of emissions by 50% for each of SO_2, BC, POA, NO_x, and VOC over East Asia (domain- and period-averaged). The boxes show ΔM for BASE simulations, and the lines show ΔDRE_{TOA} for BASE (red) and SIMPLE (blue) simulations. We used the simulation results over the inner domain (Figure S1).

dependent on OH concentrations (compared with traditional OA schemes) because of the oxidation of S/IVOCs and the resulting changes of gas-aerosol partitioning.

When OA formation is calculated without the S/IVOCs oxidation processes, the change in OA concentrations by the reduction of NO_x emissions is almost negligible in our simulations. When primary IVOC emissions are ignored in the BASE simulation, the change in OA concentrations (due to the reduction of NO_x emissions by 50%) is reduced by 40% (from 1.7 to 1.0 $\mu g\,m^{-3}$). These results show that the response of OA concentrations to changes of NO_x emissions is sensitive to the highly uncertain parameters of S/IVOC emissions and their oxidation processes. Reducing their uncertainties is therefore important to evaluate gas-oxidant-aerosol coupling accurately.

Based on these simulated responses of aerosols to reductions in emissions, we calculate the corresponding changes in direct aerosol radiative effect at the top of the atmosphere under clear-sky conditions (ΔDRE_{TOA}; Figure 2). The absolute values of ΔDRE_{TOA} in the BASE simulations are larger by 50–100% than those in the SIMPLE simulations for the emissions of BC, POA, and NO_x (increases of 68%, 49%, and 103%, respectively). We attribute the difference of the estimated ΔDRE_{TOA} for BC emissions to the different treatments of BC absorption enhancement for the BASE and SIMPLE simulations. The difference in ΔDRE_{TOA} for POA, NO_x, and VOC emissions can be explained by the treatment of OA formation processes. These results clearly show the importance of OA formation and BC aging processes in obtaining accurate estimates of aerosol responses to changes in emissions.

If gas-oxidant-aerosol coupling is not considered, the responses of ΔM and ΔDRE_{TOA} to the reduction of NO_x emissions will be much smaller because the changes of sulfate and OA concentrations are limited if both precursor (SO_2, VOC, and S/IVOCs) and oxidant (OH, O_3, and H_2O_2) concentrations do not change. This result suggests that the responses of aerosols to changes in emissions change dramatically when gas-oxidant-aerosol coupling is included in the simulations. Thus, including this coupling in simulations will be important to the formulation of effective emission reduction strategies over East Asia.

Figure 3 shows the distributions of ΔM at 1 km and ΔDRE_{TOA} due to the reductions of emissions by 50%. The distributions of ΔM for SO_2 and POA emissions generally reflect the distributions of sulfate and OA mass concentrations, respectively. The ΔM for SO_2 emissions is largest over northern and central China (Figure 3e); the ΔM for POA emissions is also large over southern China and Southeast Asia (Figure 3g). The distributions of ΔM for NO_x emissions are explained by a combination of the distributions for SO_2 and OA emissions (Figure 3a). The results show that aerosol mass concentrations are most sensitive to changes in NO_x (POA) emissions over northern and central China and outflow regions such as Korea and Japan (over southern China and Southeast Asia) in our simulations. The values of ΔM for VOC emissions are positive over China and Southeast Asia and negative over the outflow regions. The distributions are determined by the reduction of OA over China and outflow regions (lower VOC emissions) and the enhancement of inorganic aerosols (higher OH concentrations) (Figure S4). The change of OA is positive over Southeast Asia and negative over China and outflow regions (Figure S4a); although oxygenated POA is enhanced, POA and anthropogenic and biogenic secondary OA are reduced by the reductions of VOC emissions (as shown above).

The distributions of ΔDRE_{TOA} reflect aerosol concentrations over all altitudes. The result that values of ΔDRE_{TOA} are high at lower latitudes (20–30°N) for NO_x and POA emissions (Figures 3b and 3h) is consistent with the distributions of changes in aerosol optical depth (AOD) by the 50% reduction of emissions (Figure S5). The distributions of ΔDRE_{TOA} are different from the distributions of ΔM likely because the mechanism of upward transport of aerosols is different between lower and higher latitudes; aerosols at lower latitudes are transported upward mainly by convection, and the peak concentration occurs at high altitudes [e.g., *Matsui et al*., 2013c; *Oshima et al*., 2013].

3.2. Aerosol Responses Using Emissions From the Past to the Future

Figure 4 shows oxidant concentrations (at an altitude of 1 km), aerosol mass concentrations (at an altitude of 1 km), optical parameters (at a wavelength of 600 nm), and radiative effects over East Asia from 1850 and 2100 simulated with historic and $RCP_{2.6}$ emissions (simulations using $RCP_{4.5}$, $RCP_{6.0}$, and $RCP_{8.5}$ emissions are shown in Figure S6). Comparison of the results of the BASE and SIMPLE simulations shows that OA concentrations in the SIMPLE simulations are lower than those in the BASE simulations (by 50–60% during 2000–2100). The AOD differs for these two simulations, mainly because of the difference in OA

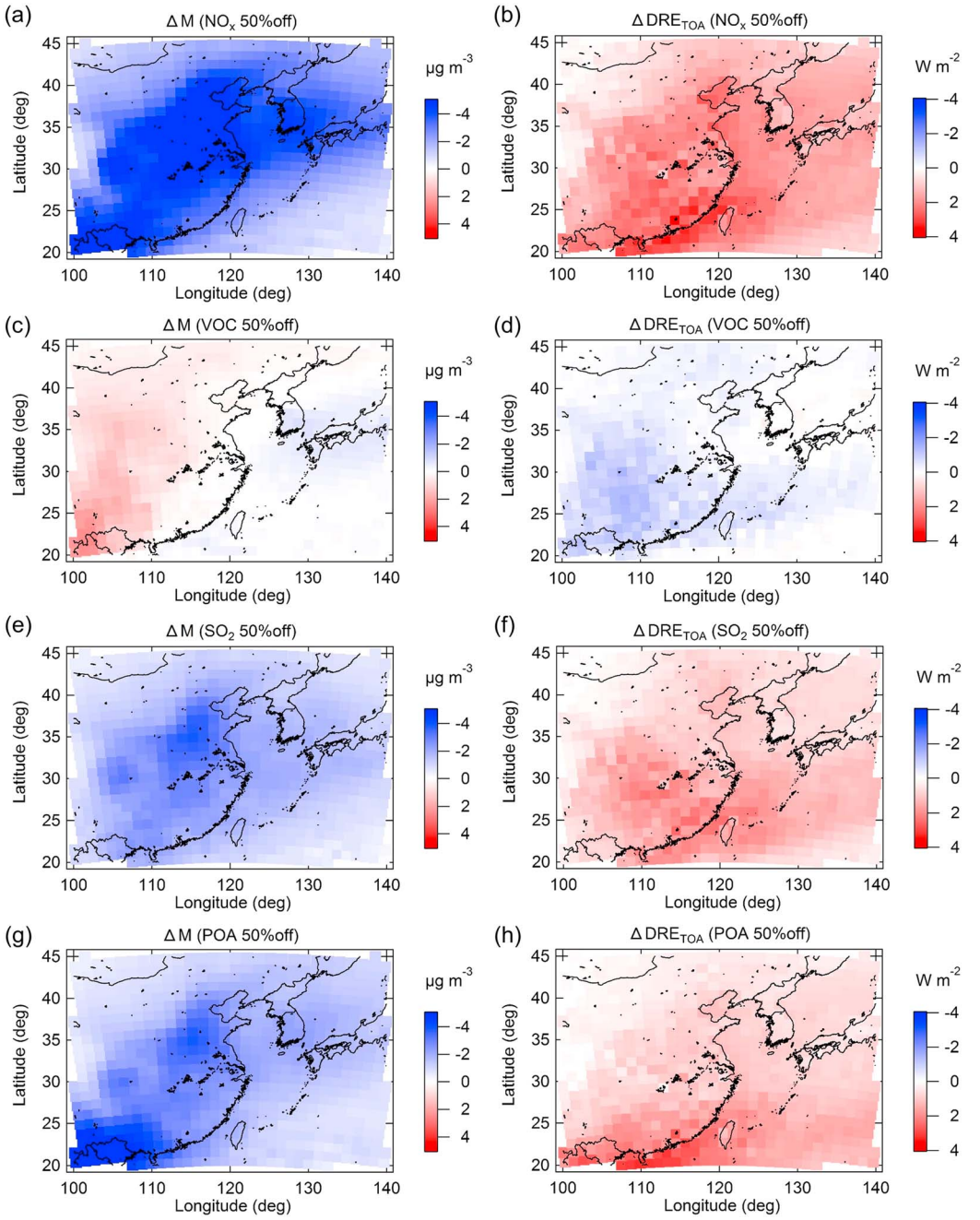

Figure 3. Spatial distributions of ΔM at an altitude of 1 km and ΔDRE_{TOA} by 50% reductions of emissions.

concentrations. Absorption AOD (AAOD) in the SIMPLE simulations is underestimated, mostly because of the treatment of BC absorption enhancement. The aerosol direct radiative effects under clear-sky conditions at the surface (DRE_{surf}) and at the top of the atmosphere (DRE_{TOA}) are also sensitive to the treatment of OA formation and BC aging processes during 1850–2100. These results show the importance of these processes in estimating impacts of aerosols on climate from the past to the future over East Asia.

We conducted sensitivity simulations to understand the impact of the increase of NO_x emissions from 1850 on aerosol parameters through gas-oxidant-aerosol coupling processes. The BASE_NOx1850 (SIMPLE_NOx1850) simulations are the same as the BASE (SIMPLE) simulations, except for the treatment of emission data. In the BASE_NOx1850 and SIMPLE_NOx1850 simulations, emission data from 1850 to 2100

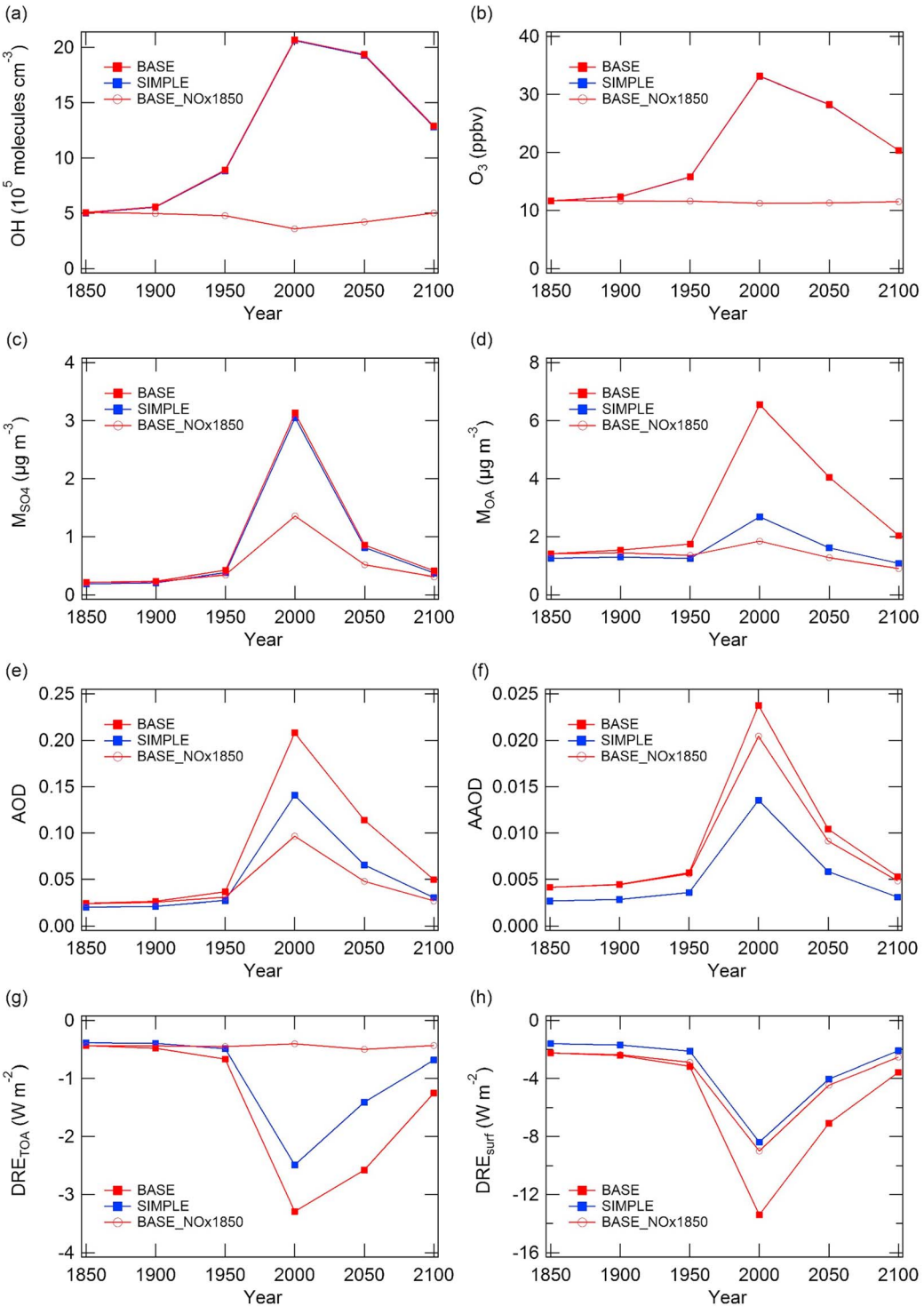

Figure 4. Simulation results (domain- and period-averaged) using emissions from 1850 to 2100 ($RCP_{2.6}$ for 2050 and 2100) and meteorological inputs in 2009: (a) OH concentrations (at 1 km altitude), (b) O_3 concentrations (at 1 km altitude), (c) sulfate mass concentrations (at 1 km altitude), (d) OA mass concentrations (at 1 km altitude), (e) column AOD, (f) column AAOD, (g) DRE_{TOA}, and (h) DRE_{surf}.

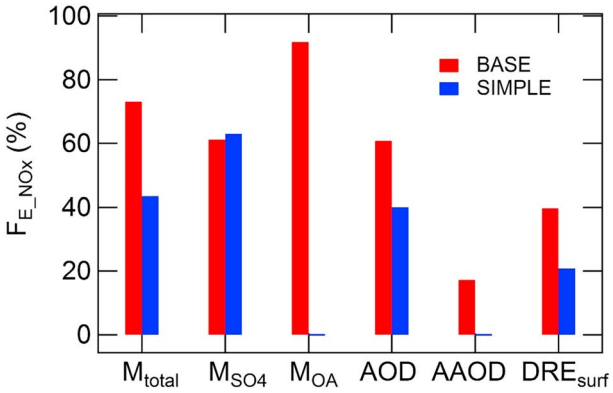

Figure 5. The contributions of the increase of NO_x emissions from 1850 to 2000 to the enhancement of aerosol parameters from 1850 to 2000 (F_{E_NOx}) for total, sulfate, and OA mass concentrations at an altitude of 1 km and for AOD, AAOD, and DRE_{surf} (averaged over the simulated domain and period). Equation (1) gives the definition of F_{E_NOx}.

are used for all gaseous and aerosol species, with the exception of NO_x. The NO_x emissions for 1850 are used for all simulations in other years. Comparison of the results of the BASE and BASE_NOx1850 simulations shows that O_3 and OH concentrations in the BASE simulations increase considerably (by factors of 2.8 and 4.1, respectively) over East Asia from 1850 to 2000 (Figures 4a, 4b, and S7) as a result of increases of NO_x emissions by a factor of 5 (Table S1). These increases of O_3 and OH are generally consistent with the results of previous studies [*Wang and Jacob*, 1998; *Murray et al.*, 2014], although our simulations produce much greater increases. *Wang and Jacob* [1998] estimated that O_3 and OH concentrations in the lower troposphere increased by more than 100% and 60%, respectively, in the northern hemisphere midlatitudes from preindustrial times to the present, whereas they estimated that global-averaged OH concentrations decreased by 9% since preindustrial times. H_2O_2 and HO_2 concentrations in the BASE simulation also increase by factors of 2.0 and 1.6, respectively, from 1850 to 2000.

The simulated increase of oxidant concentrations causes increases in OA and sulfate concentrations of 110–250% in 2000 and 30–130% in 2100, and it causes increases in AOD of 115% in 2000 and 85% in 2100 (Figures 4c–4e). AAOD increases by 16% in 2000 and by 9% in 2100 because BC absorption is enhanced by increases in coating species (sulfate and OA) (Figure 4f). The absolute values of DRE_{surf} are also enhanced by 49% in 2000 and 40% in 2100 (Figure 4h). The change in DRE_{TOA} from 1850 to 2000 is an order of magnitude smaller for the BASE_NOx1850 simulations ($-0.4\,W\,m^{-2}$) than for the BASE simulations ($-3.3\,W\,m^{-2}$) (Figure 4g) because negative DRE_{TOA} changes due to inorganic and organic aerosols are mostly canceled by positive DRE_{TOA} changes due to BC in the BASE_NOx1850 simulations. The increase of NO_x concentrations enhances inorganic and organic aerosol concentrations, which leads to large negative changes of DRE_{TOA} in the BASE simulations.

An important conclusion is that the increase of NO_x emissions since preindustrial times may have contributed considerably to the increase of aerosol concentrations and radiative parameters since preindustrial times as a result of the formation of oxidants such as OH and O_3. We calculate the contribution of the increase of NO_x emissions to the enhancement of aerosol parameters from 1850 to 2000 (F_{E_NOx}) with the following equation:

$$F_{E\_Nox,P} = \frac{C_{P,2000,BASE} - C_{P,2000,BASE\_NOx1850}}{C_{P,2000,BASE} - C_{P,1850,BASE}} \quad (1)$$

where $C_{P,Y,S}$ is the domain- and period-averaged concentration or value of parameter P for year Y (2000 or 1850) and for simulation S (BASE or BASE_NOx1850). The values of F_{E_NOx} for the SIMPLE simulations are also calculated with equation (1) by using the SIMPLE and SIMPLE_NOx1850 simulations. The F_{E_NOx} values in the BASE simulations are estimated to be 73% for total mass concentrations (particulate matter less than 2.5 μm in diameter (PM2.5)), 61% for sulfate mass concentrations, 92% for OA mass concentrations, 61% for AOD, 17% for AAOD, and 39% for DRE_{surf} (Figure 5). These results show the importance of changes of NO_x emissions from preindustrial times when simulating aerosol concentrations and radiative effects at the present time. The results also suggest that reducing NO_x emissions would be an effective way to reduce aerosol concentrations over East Asia. The comparison of F_{E_NOx} between the BASE and SIMPLE simulations shows that consideration of OA formation and BC aging processes enhances the values of F_{E_NOx} by 15–30% for $PM_{2.5}$, AOD, AAOD, and DRE_{surf} and by 90% for OA (Figure 5). The representation of these aerosol processes is therefore important for accurate estimation of NO_x contributions through gas-oxidant-aerosol coupling processes.

The results presented here are based on 1 month simulations using meteorological inputs in 2009. Because there are several limitations to our simulations, further studies will be needed in the future.

4. Summary

In this study, we quantified the sensitivity and complex responses of aerosols to changes in emissions over East Asia by using simulations that took into account detailed microphysical and chemical processes, including gas-oxidant-aerosol coupling, OA and nitrate formation, and BC aging processes.

The responses of aerosols to reductions of NO_x emissions were complex and changed dramatically when gas-oxidant-aerosol coupling was included in the simulations. A 50% reduction of NO_x emissions considerably reduced the concentrations of OH (by 40%), O_3 (by 30%), sulfate (by 24%), and OA (by 30%) over the simulation domain in East Asia. These reductions occurred because oxidant concentrations were suppressed by the reduction of NO_x emissions, and the lower oxidant concentrations slowed both the conversion rate of SO_2 to sulfate and the aging speed of S/IVOCs. Because the response of OA to changes of NO_x emissions was sensitive to the treatment of S/IVOC emissions and their oxidation processes, reducing the uncertainties in these treatments is important to evaluate gas-oxidant-aerosol processes accurately.

The results of the responses of the aerosol direct radiative effect (ΔDRE_{TOA}) to reductions of emissions clearly showed the importance of OA formation and BC aging processes in obtaining accurate estimates of aerosol responses to changes in emissions. The absolute values of ΔDRE_{TOA} in the BASE simulations were about twice the magnitude of those in the SIMPLE simulations for the emissions of BC, POA, and NO_x (increases of 68%, 49%, and 103%, respectively).

Sensitivity simulations using emissions from 1850 to 2000 showed that O_3 and OH concentrations increased considerably (by factors of 2.8 and 4.1, respectively) over East Asia from 1850 to 2000 as a result of the increase of NO_x emissions after 1850. The contributions of the increase of NO_x emissions to the enhancement of aerosol parameters from 1850 to 2000 (F_{E_NOx}) were very large because of gas-oxidant-aerosol coupling processes. The values of F_{E_NOx} in the BASE simulations were estimated to be 60–90% for $PM_{2.5}$, sulfate, and OA mass concentrations; 61% for AOD; 17% for AAOD; and 39% for DRE_{surf}. The results suggest that reducing NO_x emissions would be an effective way to reduce aerosol concentrations over East Asia. Because the values of F_{E_NOx} were much smaller in the SIMPLE simulations (40% for $PM_{2.5}$ and AOD, 20% for DRE_{surf}, and 0% for OA mass concentrations and AAOD), the importance of NO_x emissions depends on the representation of aerosol processes in the model.

Our results suggest the importance of simultaneous simulation of gas-oxidant-aerosol coupling and detailed aerosol processes, such as OA formation (including S/IVOCs emissions and their oxidation rates) and BC aging processes, for the assessment of emission reduction strategies such as BC mitigation and aerosol reduction policies in East Asia. Because whether NO_x emissions in China increase or decrease in the future depends on the policy scenario selected [*Ohara et al*., 2007; *Xing et al*., 2011; *Zhao et al*., 2013], an understanding of the impact of NO_x emissions on aerosol formation through changes in oxidant concentrations will be a key to evaluating emission reduction strategies.

Acknowledgments

H. Matsui was supported by the Japan Society for the Promotion of Science (JSPS) Postdoctoral Fellowships for Research Abroad. This work was supported by the Ministry of Education, Culture, Sports, Science, and Technology and the Japan Society for the Promotion of Science (MEXT/JSPS), KAKENHI grant numbers 26740014 and 26241003 and MEXT Green Network of Excellence (GRENE) and Arctic Challenge for Sustainability (ArCS) projects. This work was also supported by the environment research and technology development fund of the Ministry of the Environment, Japan (2-1403). The model simulations were conducted using the MSTSC super computer system at the Japan Agency for Marine-Earth Science and Technology. Data can be obtained by contacting H. Matsui (matsui@nagoya-u.jp). The authors thank the two reviewers of this manuscript for their useful suggestions.

References

Abdul-Razzak, H., and S. J. Ghan (2000), A parameterization of aerosol activation: 2. Multiple aerosol types, *J. Geophys. Res.*, *105*, 6837–6844, doi:10.1029/1999JD901161.

Ahmadov, R., et al. (2012), A volatility basis set model for summertime secondary organic aerosols over the eastern United States in 2006, *J. Geophys. Res.*, *117*, D06301, doi:10.1029/2011JD016831.

Bauer, S. E., A. Ault, and K. A. Prather (2013), Evaluation of aerosol mixing state classes in the GISS modelE-MATRIX climate model using single-particle mass spectrometry measurements, *J. Geophys. Res. Atmos.*, *118*, 9834–9844, doi:10.1002/jgrd.50700.

Bell, N., D. Koch, and D. T. Shindell (2005), Impacts of chemistry-aerosol coupling on tropospheric ozone and sulfate simulations in a general circulation model, *J. Geophys. Res.*, *110*, D14305, doi:10.1029/2004JD005538.

Berglen, T. F., T. K. Berntsen, I. S. A. Isaksen, and J. K. Sundet (2004), A global model of the coupled sulfur/oxidant chemistry in the troposphere: The sulfur cycle, *J. Geophys. Res.*, *109*, D19310, doi:10.1029/2003JD003948.

Bohren, C. F., and D. R. Huffman (1998), *Absorption and Scattering of Light by Small Particles*, 530 pp., John Wiley, Hoboken.

Bond, T. C., G. Habib, and R. W. Bergstrom (2006), Limitations in the enhancement of visible light absorption due to mixing state, *J. Geophys. Res.*, *111*, D20211, doi:10.1029/2006JD007315.

Bond, T. C., et al. (2013), Bounding the role of black carbon in the climate system: A scientific assessment, *J. Geophys. Res. Atmos.*, *118*, 5380–5552, doi:10.1002/jgrd.50171.

Boucher, O., et al. (2013), Clouds and Aerosols, in *Climate Change 2013: The Physical Science Basis. Contribution of Working Group I to the Fifth Assessment Report of the Intergovernmental Panel on Climate Change*, edited by T. F. Stocker, Cambridge Univ. Press, New York.

Carter, W. P. L. (2000), Documentation of the SAPRC-99 Chemical Mechanism for VOC Reactivity Assessment, Report to the California Air Resources Board. College of Eng., Cent. for Environ. Res. and Technol., Univ. of Calif. at Riverside, Calif., Contracts 92–329 and 95–308. [Available at http://www.cert.ucr.edu/~carter/reactdat.htm, Accessed 25 Apr. 2016.]

Chan, C. K., and X. Yao (2008), Air pollution in mega cities in China, *Atmos. Environ.*, *42*, 1–42.

Chou, M. D. (1992), A solar radiation model for use in climate studies, *J. Atmos. Sci.*, *49*, 762–772.

Easter, R. C., S. J. Ghan, Y. Zhang, R. D. Saylor, E. G. Chapman, N. S. Laulainen, H. Abdul-Razzak, L. R. Leung, X. Bian, and R. A. Zaveri (2004), MIRAGE: Model description and evaluation of aerosols and trace gases, *J. Geophys. Res.*, *109*, D20210, doi:10.1029/2004JD004571.

Ervens, B., B. J. Turpin, and R. J. Weber (2011), Secondary organic aerosol formation in cloud droplets and aqueous particles (aqSOA): A review of laboratory, field and model studies, *Atmos. Chem. Phys.*, *11*, 11,069–11,102.

Ervens, B., A. Sorooshian, Y. B. Lim, and B. J. Turpin (2014), Key parameters controlling OH-initiated formation of secondary organic aerosol in the aqueous phase (aqSOA), *J. Geophys. Res. Atmos.*, *119*, 3997–4016, doi:10.1002/2013JD021021.

Fahey, K. M., and S. N. Pandis (2001), Optimizing model performance: Variable size resolution in cloud chemistry modeling, *Atmos. Environ.*, *35*, 4471–4478.

Fast, J. D., W. I. Gustafson Jr., R. C. Easter, R. A. Zaveri, J. C. Barnard, E. G. Chapman, G. A. Grell, and S. E. Peckham (2006), Evolution of ozone, particulates, and aerosol direct radiative forcing in the vicinity of Houston using a fully coupled meteorology-chemistry-aerosol model, *J. Geophys. Res.*, *111*, D21305, doi:10.1029/2005JD006721.

Fry, M. M., et al. (2012), The influence of ozone precursor emissions from four world regions on tropospheric composition and radiative climate forcing, *J. Geophys. Res.*, *117*, D07306, doi:10.1029/2011JD017134.

Guenther, A., T. Karl, P. Harley, C. Wiedinmyer, P. I. Palmer, and C. Geron (2006), Estimates of global terrestrial isoprene emissions using MEGAN (Model of Emissions of Gases and Aerosols from Nature), *Atmos. Chem. Phys.*, *6*, 3181–3210.

Hauglustaine, D. A., Y. Balkanski, and M. Schulz (2014), A global model simulation of present and future nitrate aerosols and their direct radiative forcing of climate, *Atmos. Chem. Phys.*, *14*, 11,031–11,063.

Heald, C. L., D. J. Jacob, R. J. Park, L. M. Russell, B. J. Huebert, J. H. Seinfeld, H. Liao, and R. J. Weber (2005), A large organic aerosol source in the free troposphere missing from current models, *Geophys. Res. Lett.*, *32*, L18809, doi:10.1029/2005GL023831.

He, C., K.-N. Liou, Y. Takano, R. Zhang, M. Levy Zamora, P. Yang, Q. Li, and L. R. Leung (2015), Variation of the radiative properties during black carbon aging: theoretical and experimental intercomparison, *Atmos. Chem. Phys.*, *15*, 11,967–11,980.

He, C., Q. Li, K.-N. Liou, L. Qi, S. Tao, and J. P. Schwarz (2016), Microphysics-based black carbon aging in a global CTM: constraints from HIPPO observations and implications for global black carbon budget, *Atmos. Chem. Phys.*, *16*, 3077–3098.

Hodzic, A., J. L. Jimenez, S. Madronich, M. R. Canagaratna, R. F. DeCarlo, L. Kleinman, and J. Fast (2010), Modeling organic aerosols in a megacity: Potential contribution of semi-volatile and intermediate volatility primary organic compounds to secondary organic aerosol formation, *Atmos. Chem. Phys.*, *10*, 5491–5514.

Jacobson, M. Z. (2002), Control of fossil-fuel particulate black carbon and organic matter, possibly the most effective method of slowing global warming, *J. Geophys. Res.*, *107*(D19), 4410, doi:10.1029/2001JD001376.

Jacobson, M. Z., R. P. Turco, E. J. Jensen, and O. B. Toon (1994), Modeling coagulation among particles of different composition and size, *Atmos. Environ.*, *28*, 1327–1338.

Kanaya, Y., R. Cao, H. Akimoto, M. Fukuda, Y. Komazaki, Y. Yokouchi, M. Koike, H. Tanimoto, N. Takegawa, and Y. Kondo (2007), Urban photochemistry in central Tokyo: 1. Observed and modeled OH and HO2 radical concentrations during the winter and summer of 2004, *J. Geophys. Res.*, *112*, D21312, doi:10.1029/2007JD008670.

Kondo, Y., et al. (2010), Formation and transport of aerosols in Tokyo in relation to their physical and chemical properties: A review, *J. Meteor. Soc. Japan*, *88*, 597–624.

Kondo, Y., N. Oshima, M. Kajino, R. Mikami, N. Moteki, N. Takegawa, R. L. Verma, Y. Kajii, S. Kato, and A. Takami (2011), Emissions of black carbon in East Asia estimated from observations at a remote site in the East China Sea, *J. Geophys. Res.*, *116*, D16201, doi:10.1029/2011JD015637.

Kulmala, M., K. E. J. Lehtinen, and A. Laaksonen (2006), Cluster activation theory as an explanation of the linear dependence between formation rate of 3 nm particles and sulphuric acid concentration, *Atmos. Chem. Phys.*, *6*, 787–793.

Lamarque, J.-F., et al. (2010), Historical (1850–2000) gridded anthropogenic and biomass burning emissions of reactive gases and aerosols: methodology and application, *Atmos. Chem. Phys.*, *10*, 7017–7039.

Liu, J., L. W. Horowitz, S. Fan, A. G. Carlton, and H. Levy II (2012), Global in-cloud production of secondary organic aerosols: Implementation of a detailed chemical mechanism in the GFDL atmospheric model AM3, *J. Geophys. Res.*, *117*, D15303, doi:10.1029/2012JD017838.

Liu, X., P.-L. Ma, H. Wang, S. Tilmes, B. Singh, R. C. Easter, S. J. Ghan, and P. J. Rasch (2016), Description and evaluation of a new four-mode version of the Modal Aerosol Module (MAM4) within version 5.3 of the Community Atmosphere Model, *Geosci. Model Dev.*, *9*, 505–522.

Matsui, H. (2016a), Black carbon simulations using a size- and mixing-state-resolved three-dimensional model: 1. Radiative effects and their uncertainties, *J. Geophys. Res. Atmos.*, *121*, 1793–1807, doi:10.1002/2015JD023998.

Matsui, H. (2016b), Black carbon simulations using a size- and mixing-state-resolved three-dimensional model: 2. Aging timescale and its impact over East Asia, *J. Geophys. Res. Atmos.*, *121*, 1808–1821, doi:10.1002/2015JD023999.

Matsui, H., M. Koike, N. Takegawa, Y. Kondo, R. J. Griffin, Y. Miyazaki, Y. Yokouchi, and T. Ohara (2009), Secondary organic aerosol formation in urban air: Temporal variations and possible contributions from unidentified hydrocarbons, *J. Geophys. Res.*, *114*, D04201, doi:10.1029/2008JD010164.

Matsui, H., M. Koike, Y. Kondo, N. Takegawa, A. Wiedensohler, J. D. Fast, and R. A. Zaveri (2011), Impact of new particle formation on the concentrations of aerosols and cloud condensation nuclei around Beijing, *J. Geophys. Res.*, *116*, D19208, doi:10.1029/2011JD016025.

Matsui, H., M. Koike, Y. Kondo, N. Moteki, J. D. Fast, and R. A. Zaveri (2013a), Development and validation of a black carbon mixing state resolved three-dimensional model: Aging processes and radiative impact, *J. Geophys. Res. Atmos.*, *118*, 2304–2326, doi:10.1029/2012JD018446.

Matsui, H., M. Koike, N. Takegawa, Y. Kondo, A. Takami, T. Takamura, S. Yoon, S.-W. Kim, H.-C. Lim, and J. D. Fast (2013b), Spatial and temporal variations of new particle formation in East Asia using an NPF-explicit WRF-Chem model: North-south contrast in new particle formation frequency, *J. Geophys. Res. Atmos.*, *118*, 11,647–11,663, doi:10.1002/jgrd.50821.

Matsui, H., M. Koike, Y. Kondo, N. Oshima, N. Moteki, Y. Kanaya, A. Takami, and M. Irwin (2013c), Seasonal variations of Asian black carbon outflow to the Pacific: Contribution from anthropogenic sources in China and biomass burning sources in Siberia and Southeast Asia, *J. Geophys. Res. Atmos.*, *118*, 9948–9967, doi:10.1002/jgrd.50702.

Matsui, H., M. Koike, Y. Kondo, J. D. Fast, and M. Takigawa (2014a), Development of an aerosol microphysical module: Aerosol Two-dimensional bin module for foRmation and Aging Simulation (ATRAS), *Atmos. Chem. Phys.*, *14*, 10,315–10,331.

Matsui, H., M. Koike, Y. Kondo, A. Takami, J. D. Fast, Y. Kanaya, and M. Takigawa (2014b), Volatility basis-set approach simulation of organic aerosol formation in East Asia: Implications for anthropogenic-biogenic interaction and controllable amounts, *Atmos. Chem. Phys.*, *14*, 9513–9535.

Murray, L. T., L. J. Mickley, J. O. Kaplan, E. D. Sofen, M. Pfeiffer, and B. Alexander (2014), Factors controlling variability in the oxidative capacity of the troposphere since the Last Glacial Maximum, *Atmos. Chem. Phys.*, *14*, 3589–3622.

Moss, R. H., et al. (2010), The next generation of scenarios for climate change research and assessment, *Nature*, *463*, 747–756.

Moteki, N., Y. Kondo, Y. Miyazaki, N. Takegawa, Y. Komazaki, G. Kurata, T. Shirai, D. R. Blake, T. Miyakawa, and M. Koike (2007), Evolution of mixing state of black carbon particles: Aircraft measurements over the western Pacific in March 2004, *Geophys. Res. Lett.*, *34*, L11803, doi:10.1029/2006GL028943.

Moteki, N., Y. Kondo, N. Oshima, N. Takegawa, M. Koike, K. Kita, H. Matsui, and M. Kajino (2012), Size dependence of wet removal of black carbon aerosols during transport from the boundary layer to the free troposphere, *Geophys. Res. Lett.*, *39*, L13802, doi:10.1029/2012GL052034.

Murphy, B. N., and S. N. Pandis (2009), Simulating the formation of semivolatile primary and secondary organic aerosol in a regional chemical transport model, *Environ. Sci. Technol.*, *43*, 4722–4728.

Ohara, T., H. Akimoto, J. Kurokawa, N. Horii, K. Yamaji, X. Yan, and T. Hayasaka (2007), An Asian emission inventory of anthropogenic emission sources for the period 1980–2020, *Atmos. Chem. Phys.*, *7*, 4419–4444.

Oshima, N., et al. (2012), Wet removal of black carbon in Asian outflow: Aerosol Radiative Forcing in East Asia (A-FORCE) aircraft campaign, *J. Geophys. Res.*, *117*, D03204, doi:10.1029/2011JD016552.

Oshima, N., M. Koike, Y. Kondo, H. Nakamura, N. Moteki, H. Matsui, N. Takegawa, and K. Kita (2013), Vertical transport mechanisms of black carbon over East Asia in spring during the A-FORCE aircraft campaign, *J. Geophys. Res. Atmos.*, *118*, 13,175–13,198, doi:10.1002/2013JD020262.

Pope, C. A., III, R. T. Burnett, M. J. Thun, E. E. Calle, D. Krewski, K. Ito, and G. D. Thurston (2002), Lung cancer, cardiopulmonary mortality, and long-term exposure to fine particulate air pollution, *J. Am. Med. Assoc.*, *287*, 1132–1141.

Ramanathan, V., and Y. Y. Xu (2010), The Copenhagen Accord for limiting global warming: Criteria, constraints, and available avenues, *Proc. Natl. Acad. Sci. U.S.A.*, *107*(18), 8055–8062.

Shindell, D. T., G. Faluvegi, D. M. Koch, G. A. Schmidt, N. Unger, and S. E. Bauer (2009), Improved attribution of climate forcing to emissions, *Science*, *326*, 716–718.

Stier, P., J. H. Seinfeld, S. Kinne, J. Feichter, and O. Boucher (2006), Impact of nonabsorbing anthropogenic aerosols on clear-sky atmospheric absorption, *J. Geophys. Res.*, *111*, D18201, doi:10.1029/2006JD007147.

Surratt, J. D., A. W. Chan, N. C. Eddingsaas, M. N. Chan, C. L. Loza, A. J. Kwan, S. P. Hersey, R. C. Flagan, P. O. Wennberg, and J. H. Seinfeld (2010), Reactive intermediates revealed in secondary organic aerosol formation from isoprene, *Proc. Natl. Acad. Sci. U.S.A.*, *107*(15), 6640–6645.

Takami, A., T. Miyoshi, A. Shimono, and S. Hatakeyama (2005), Chemical composition of fine aerosol measured by AMS at Fukue Island, Japan, during APEX period, *Atmos. Environ.*, *39*, 4913–4924.

Takami, A., T. Miyoshi, A. Shimono, N. Kaneyasu, S. Kato, Y. Kajii, and S. Hatakeyama (2007), Transport of anthropogenic aerosols from Asia and subsequent chemical transformation, *J. Geophys. Res.*, *112*, D22S31, doi:10.1029/2006JD008120.

Takegawa, N., N. Moteki, N. Oshima, M. Koike, K. Kita, A. Shimizu, N. Sugimoto, and Y. Kondo (2014), Variability of aerosol particle number concentrations observed over the western Pacific in the spring of 2009, *J. Geophys. Res. Atmos.*, *119*, 13,474–13,488, doi:10.1002/2014JD022014.

Tsigaridis, K., et al. (2014), The AeroCom evaluation and intercomparison of organic aerosol in global models, *Atmos. Chem. Phys.*, *14*, 10,845–10,895.

Tsimpidi, A. P., V. A. Karydis, M. Zavala, W. Lei, L. Molina, I. M. Ulbrich, J. L. Jimenez, and S. N. Pandis (2010), Evaluation of the volatility basis-set approach for the simulation of organic aerosol formation in the Mexico City metropolitan area, *Atmos. Chem. Phys.*, *10*, 525–546.

Tsimpidi, A. P., V. A. Karydis, M. Zavala, W. Lei, N. Bei, L. Molina, and S. N. Pandis (2011), Sources and production of organic aerosol in Mexico City: Insights from the combination of a chemical transport model (PMCAMx-2008) and measurements during MILAGRO, *Atmos. Chem. Phys.*, *11*, 5153–5168.

Utembe, S. R., M. C. Cooke, A. T. Archibald, D. E. Shallcross, R. G. Derwent, and M. E. Jenkin (2011), Simulating secondary organic aerosol in a 3-D Lagrangian chemistry transport model using the reduced Common Representative Intermediates mechanism (CRI v2-R5), *Atmos. Environ.*, *45*, 1604–1614.

Wang, J., and D. J. Jacob (1998), Anthropogenic forcing on tropospheric ozone and OH since preindustrial times, *J. Geophys. Res.*, *103*, 31,123–31,135, doi:10.1029/1998JD100004.

Wexler, A. S., F. W. Lurmann, and J. H. Seinfeld (1994), Modelling urban and regional aerosols. Part I: Model development, *Atmos. Environ.*, *28*, 531–546.

Wild, O., X. Zhu, and M. J. Prather (2000), Fast-J: Accurate simulation of in- and below-cloud photolysis in tropospheric chemical models, *J. Atmos. Chem.*, *37*, 245–282.

Xing, J., S. X. Wang, S. Chatani, C. Y. Zhang, W. Wei, J. M. Hao, Z. Klimont, J. Cofala, and M. Amann (2011), Projections of air pollutant emissions and its impacts on regional air quality in China in 2020, *Atmos. Chem. Phys.*, *11*, 3119–3136.

Xu, L., and J. E. Penner (2012), Global simulations of nitrate and ammonium aerosols and their radiative effects, *Atmos. Chem. Phys.*, *12*, 9479–9504.

Yu, H., et al. (2013), A multimodel assessment of the influence of regional anthropogenic emission reductions on aerosol direct radiative forcing and the role of intercontinental transport, *J. Geophys. Res. Atmos.*, *118*, 700–720, doi:10.1029/2012JD018148.

Zaveri, R. A., R. C. Easter, J. D. Fast, and L. K. Peters (2008), Model for Simulating Aerosol Interactions and Chemistry (MOSAIC), *J. Geophys. Res.*, *113*, D13204, doi:10.1029/2007JD008782.

Zhao, B., S. W. Wang, H. Liu, J. Y. Xu, K. Fu, Z. Klimont, J. M. Hao, K. B. He, J. Cofala, and M. Amann (2013), NOx emissions in China: Historical trends and future perspectives, *Atmos. Chem. Phys.*, *13*, 9869–9897.